Fifth International Symposium on Marine Propulsors
smp'17, Espoo, Finland, June 2017

CFD application for an icebreaker propeller design

Mikhail P. Lobachev, Timur I. Saifullin, Andrei E. Taranov, Irina G. Frolova

Krylov State Research Centre, St. Petersburg, Russian Federation

ABSTRACT

The present work describes the procedure of the propeller blade modification in order to increase its hydrodynamic and cavitation characteristics. The object of investigation is an icebreaker propeller, pre-designed according to requirements of the Russian Maritime Register of Shipping. A new form of blade section has been proposed based on the numerical simulation of two-dimensional flow around a blade profile, including the effects of cavitation.

Keywords

Computational fluid dynamic (CFD), icebreaker, propeller, cavitation, validation.

1 INTRODUCTION

An important problem of icebreaker propellers design is the choosing of blade parameters to provide less cavitation at extremely low speed and high power rates in very thick ice condition.

Until now, the practical design of icebreaker propulsor is realized using approximate methods based mostly on empirical approaches. This situation is determined by insufficient knowledge about hydrodynamic processes arising during the propeller motion at bollard pull mode. Problems which are deficiently investigated are the following:

-the hydrodynamic particularity of flow around propeller's blade at high angles of attack,

-the forming and behavior of the vortex systems near the blades as well as in the propeller's jet, especially taking into account the presence of the ship hull and adjoining propulsors of the multi-shaft vessel.

As a result of above mentioned the design of a propeller both for an icebreaker and for a high ice-class vessels is pointed firstly on the complicated ice condition where the safety and reliability prevail on the hydrodynamic efficiency. Therefore the icebreaker propellers usually have less efficiency due to the thicker blade's profiles caused by class strength requirement. That leads in turn to the downgrade of the technical and economic characteristics of the vessel, unnecessary fuel consumption, reduced propulsion efficiency in the free-water and ice-breaking modes. Sea trials and model tests of icebreaker propellers have always shown the first stage of cavitation (incipient cavitation) working at bollard pull and ice-breaking modes. In this way, the main purpose of propeller design is to exclude the second stage of cavitation (fully developed cavitation) that results in the significant propeller characteristics losses.

To ensure the absence of an extensive cavitation it is necessary to reduce the propeller's blade profile camber. However, it decreases an efficiency of the propeller in open water conditions as well as an efficiency of power processing while in ice breaking mode conditions. Therefore finding the maximum of acceptable blade profile camber excluding the extensive cavitation with a sufficient safety factor is the relevant task.

The present work describes the procedure of the propeller blade modification in order to increase its hydrodynamic and cavitation characteristics. The work was carried out at Krylov State Research Centre involving some experimental facilities; nevertheless, this paper is focused on the validation and using of CFD methods as a support to the icebreaker propeller design.

2 TWO-DIMENSIONAL FLOW AROUND PROFILE INCLUDING CAVITAION

The object of investigation is an icebreaker propeller, pre-designed according to requirements of the Russian Maritime Register of Shipping. The general view of the prototype propeller is shown in the Figure 1. The profile of its blade is shown in the Figure 2(a).

At the first stage of investigations, two new shapes of the blade's profile were suggested based on the two-dimensional simulation of the flow around the profile, including the effects of cavitation. The first modification transforms a camber, shifting it to the leading edge (Figure 2(b)), which, in theory, should slightly improve a hydrodynamic efficiency of the blade but should not change the beginning of full cavitation. The second modified profile has additionally a chamfering of suction

side on the leading edge (Figure 2(c)), which reduces the load on the blade while ice cutting (Belyashov 1993) and postpones the beginning of the second stage of cavitation as well.

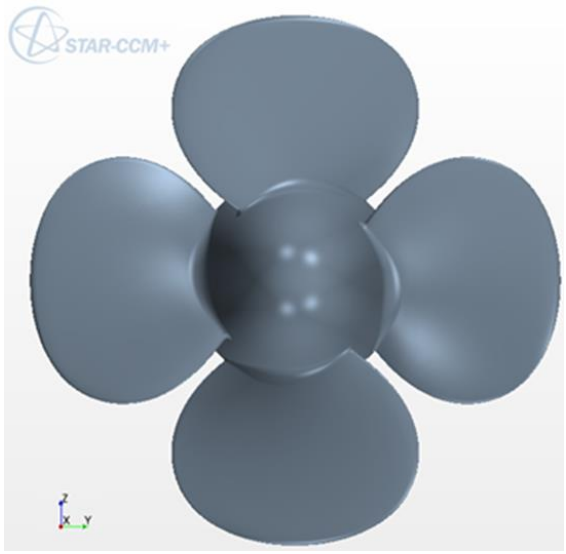

Figure 1 – The general view of the prototype propeller

Figure 2 – Blade's profile of the prototype propeller (a) and its two modifications

The numerical simulation of the cavitating flow around three shown above profiles was done using Star-CCM+ CFD package, using the k-ω SST turbulence model (Menter 1994) and Schnerr and Sauer cavitation model (Sauer 2000) for the cavitation number range of 0.375 – 4.5.

The cavitation number is calculated as follows:

$$\sigma_b = \frac{(P - P_{vap})}{\rho \cdot (n \cdot D)^2 / 2} \quad (1)$$

where n is the rate of revolution (1/s), D is the diameter of the propeller (m), ρ is the density (kg/m^3), P is the pressure (Pa), P_{vap} is the saturation pressure (taken as 2325 Pa).

The dependencies of the drag and lift coefficients as well as lift-to-drag ratio on the cavitation number are plotted in the Figures 3-5. It is clear to see that modification of the camber raises the lift-to-drag ratio (through the reducing of the drag and slight reduction of the lift) and slightly postpones the beginning of the second stage of cavitation simultaneously. The chamfering of suction side on the leading edge of prototype propeller decreases the lift-to-drag ratio but postpones distinctly the beginning of the second stage of cavitation. The beginning of the fully developed cavitation is shifted from the cavitation number 3 to 1.5. Thus, the results of the two-dimensional cavitating simulation are in agreement with theoretical assumptions. Note that raising of the angle of attack for the profile with chamfering (Figure 2 (c)) to increase the lifting force upto prototype one's leads to downgrade of its cavitation characteristics. The cavities at leading edge of investigated blade profiles are shown in the Figure 6 for different cavitation numbers.

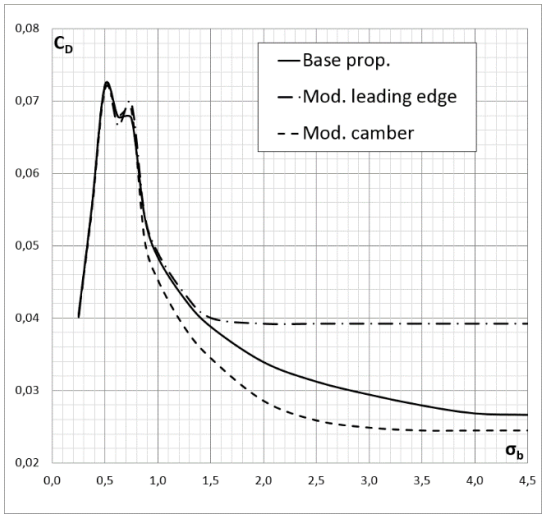

Figure 3 – Drag coefficient vs. cavitation number

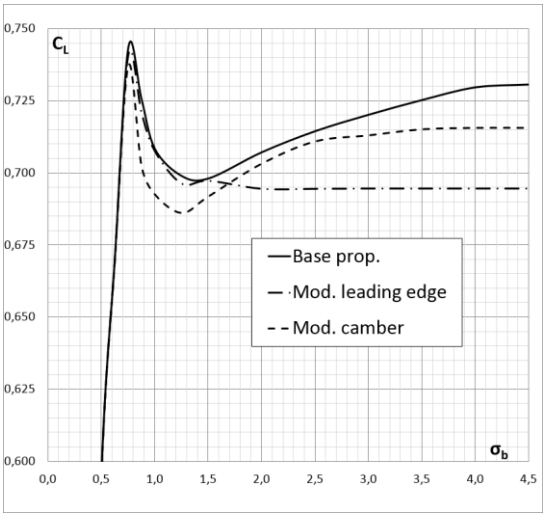

Figure 4 – Lift coefficient vs. cavitation number

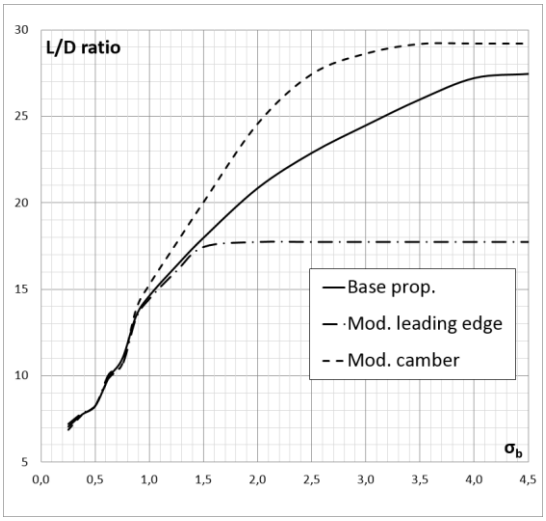

Figure 5 – Lift-to-drag ratio vs. cavitation number

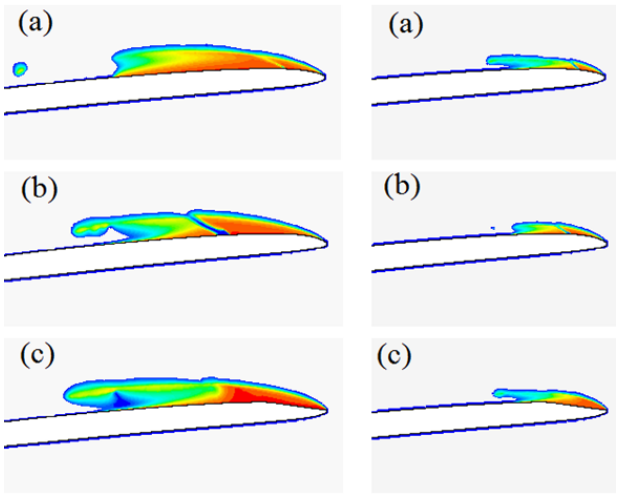

Figure 6 – Cavities at leading edge of investigated blade profiles. Cavitation number 0.875 (left) and 1.25 (right)

3 THREE-DIMENSIONAL FLOW AROUND PROPELLER INCLUDING CAVITATION

Previously obtained results were taken as input data to design modified propeller. The CAD model of the propeller was constructed using profile presented in the Figure 2(c) and was investigated by CFD methods to validate existing numerical technologies of propeller's characteristic prediction. The corresponding physical model was used in experimental tests at Krylov State Research Centre.

The commercial package STAR-CCM+ is used at Krylov State Research Centre for the numerical simulation of the viscous flow around the model of propellers. The characteristics of the viscous fluid flow are found by solving the unsteady Reynold's equations, closed by the turbulence model using finite volume elements method. It is possible to use a Detached Eddy Simulation (DES) approach within STAR-CCM+. In some cases, it is necessary to use DES to properly simulate cavitating flows. The STAR-CCM+ package includes a mesh generator, which produces polyhedral or hexahedral computational grids with prismatic sublayers near the surfaces.

The low-Reynolds version of the k-ω SST turbulence model (Menter 1994) is used in the present CFD study for the "open water" condition and the DES turbulence approach based on the k-ω SST model (Shur et al 2008) used for the bollard pull modes, where cavitation is noticeably developed.

Multiphase flow of water and vapor mixture is realized using Volume of Fluid (VoF) method (Hirt & Nichols 1981). A source term is added to the equation according to Rayleigh–Plesset model (Rayleigh 1917) in order to take into account the interaction between phases including bubble generation and their collapse. Additionally the surface tension effects are included. Numerical modeling of the flow is performed using second order temporal and spatial discretization schemes.

Both phases have constant density: 1000 kg/m^3 for the water and 0.595 kg/m^3 for the vapor. Dynamic viscosity of the water is 0.001141 Pa*s and 1.268*10^{-5} Pa*s for the vapor. Saturation pressure is constant and equal to the 2325 Pa.

The computational domain is cylinder with rotating cylindrical subregion where the propeller is placed. Free flow condition (P = 0) is set as boundary condition in the middle part of the outlet. Constant value of the inflow velocity, turbulence intensity and turbulence viscosity ratio are set as boundary conditions on rest of the outlet and on the inlet. The slip wall condition is set on the external domain surface. It prevents the leakage of the liquid from the computational domain influenced by the gravity force.

Hexahedral computational grid with prismatic sublayers produced by STAR-CCM+ built-in mesh generator contains about 9-12 million of cells. Prismatic area consists of 28 layers. The thickness of the first layer (2.0*10^{-6} m) is chosen to satisfy low-Reynolds turbulence model requirement on the dimensionless wall distance Y$^+$. Distribution of the dimensionless wall distance Y$^+$ is plotted in the Figure 7. It is clear to see, that requirements of the low-Reynolds turbulence model are satisfied; Y+ is basically less than 0.5 increasing up to 0.8-0.9 on the propeller's edges.

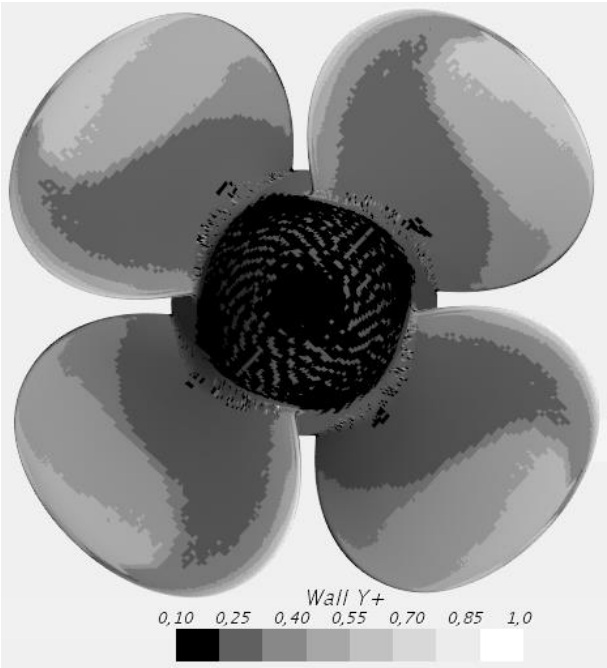

Figure 7 – Distribution of the dimensionless wall distance

The "open water" performance diagram for the model of the prototype propeller is plotted in the Figure 8 versus advance coefficient J. The comparison of the results obtained from the CFD with the experimental data shows that existing technology predicts the hydrodynamic characteristics of the propeller in the model scale with high accuracy provided that laminar-turbulent transition model γ-Re$_\theta$ (Menter et al 2006) is used. More about using of the laminar-turbulent transition model for the prediction of the

propeller characteristics see in papers (Taranov & Lobachev 2015), (Taranov 2015).

Thrust (K_T) and torque (K_Q) coefficients are defined using following formulae:

$$K_T = \frac{T}{\rho \cdot n^2 \cdot D^4} \quad (2)$$

$$K_Q = \frac{Q}{\rho \cdot n^2 \cdot D^5} \quad (3)$$

where T is the propeller thrust (N) and Q is the propeller torque (N*m).

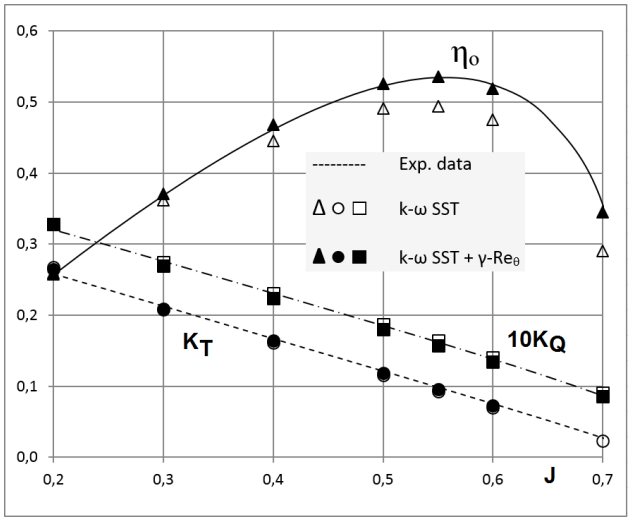

Figure 8 – "Open water" performance diagram of the prototype propeller in the model scale

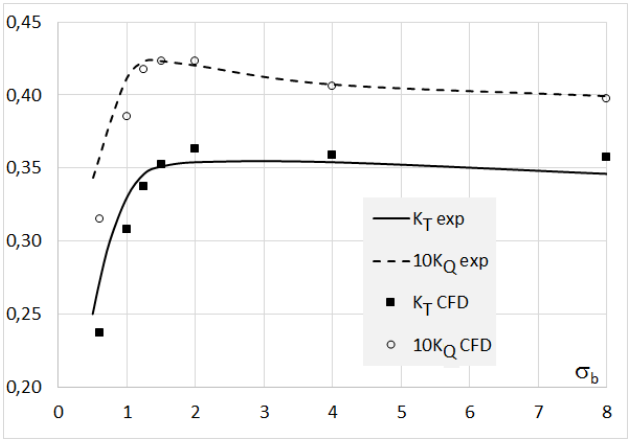

Figure 9 – Thrust and torque coefficients of the prototype propeller's model at the bollard pull modes

Thrust and torque coefficients as variation of the cavitation number are plotted in the Figure 9 for the prototype propeller working at the bollard pull mode. The accuracy of presented hydrodynamic characteristics obtained with DES approach is rather good, within 2-7% range for the cavitation numbers corresponding to the second stage of cavitation, wherein accuracy lowers with decreasing of the cavitation number. In other words, the CFD prediction shows less accuracy in fully developed cavitation modes, which have not practical interest and not taken into account during design process. It should be noted that pointed-above accuracy of the numerical prediction of the propeller's model characteristics can only be achieved, taking into account all flow affecting elements of experimental facility, i.e. fairings, shafting, dynamometer etc.

Figure 10 represents the cavities around the model of the prototype propeller corresponding to the first (top) and the second (bottom) stages of cavitation.

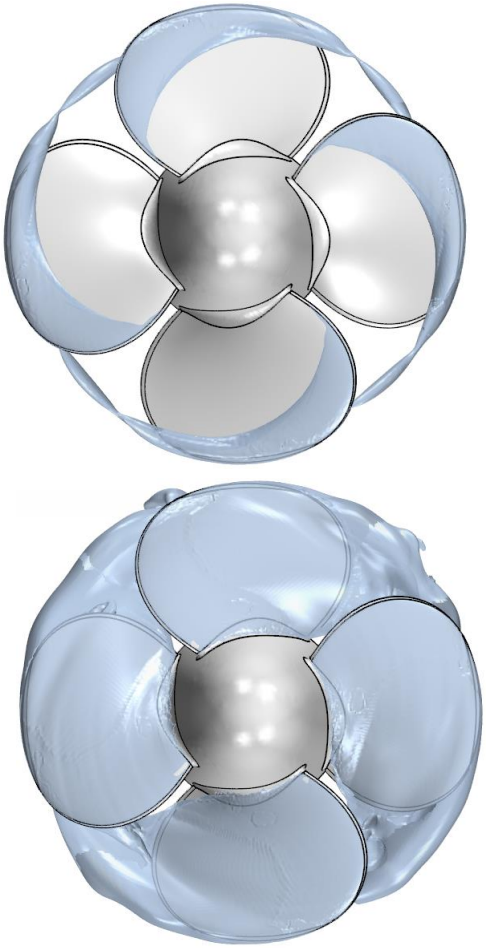

Figure 10 - Cavities around the model of the prototype propeller. Bollard pull mode, cavitation number: 2.0 (top) and 0.6 (bottom)

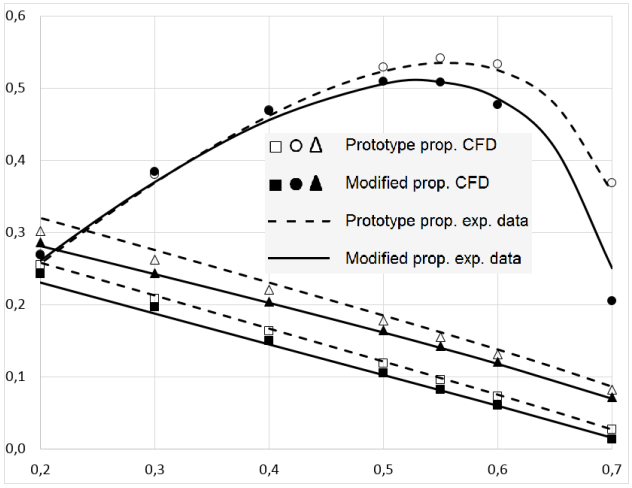

Figure 11 – Hydrodynamic efficiency of the prototype and modified propeller's models

Comparison between characteristics of the prototype and modified propeller's models shown in the Figures 11 and

12 allows concluding that modified propeller's model has a little less thrust, including the bollard pull modes, and less efficiency at the full ahead mode. The cavitation number corresponding the second stage of the cavitation remains unchanged comparing with prototype propeller's model. In the case of subsequent increasing of thrust for the modified propeller upto the level of the prototype one's, its cavitation characteristics will be lowered a little. However, the full redesigning of the propeller is beyond the scope of this task.

At the same time, modified propeller is suitable for the ice milling that should increase its lifetime. Obtained results suggest that prediction of the hydrodynamic and cavitation characteristics of the propellers in model scale based on two-dimensional numerical modelling does not reflect the complexity of the flow around the propeller in a wide range of advance coefficient – from the full ahead mode to the bollard pull mode. Simultaneously the results of the three-dimensional numerical simulation are consistent with the experimental data with high accuracy.

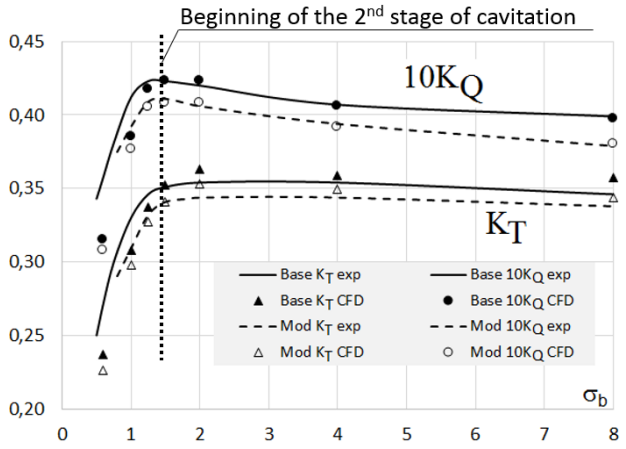

Figure 12 – Hydrodynamic and cavitation characteristics of the prototype and modified propeller's models at bollard pull modes

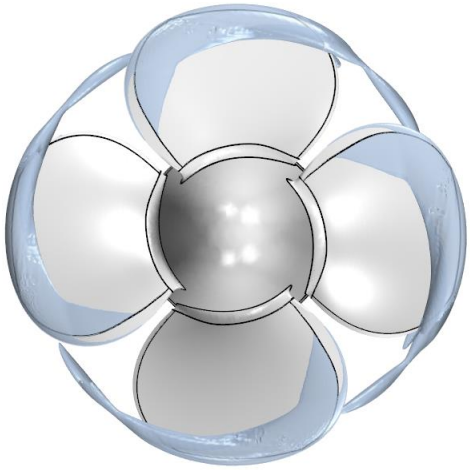

Figure 13 - Cavities around the model of the modified propeller. Bollard pull mode, cavitation number - 2.0

4 CONCLUSION

Analysis of performed model tests and CFD simulations shows that not all the aims of the work have been achieved. Modified propeller has 5% efficiency loss compared to prototype propeller at maximum speed conditions. The main impact of the blade profile modification is that cavitation type on the pressure side of the blade has been changed. There is a trailing vortex observed from the pressure side of the base blade, while on the modified blade a sheet cavitation appears on the radii r/R = 0,35-0,50 (Figure 13).

As predicted, the change of the blade camber and presence of chamfering of the suction side of the leading edge does not affect the cavitation number corresponding to the second stage of cavitation (without additional actions to preserve thrust of the propeller). Comparative analysis of hydrodynamic characteristics in the bollard pull mode showed that the changes in the geometry of the propeller led to a slight increase of the static thrust coefficient

$$K_T/(\pi \cdot K_Q^{2/3} \cdot 2^{1/3})$$

(+ 0.2%), which describes the efficiency of the propeller in the bollard pull mode, excluding the impact of the hull. However, the presence of chamfering is most important advantage of the modified propeller. It reduces the risk of blade breakage while operation in ice cutting conditions and thereby increases the safety of navigation of the icebreaker.

A significant positive result of the present work is that the validation of numerical simulations by comparison with experimental data showed a good accuracy of the supercomputer technologies existed at Krylov State Research Centre for both hydrodynamic and cavitation characteristics prediction, including the beginning of the second stage of cavitation (when reducing of hydrodynamic characteristics occurs).

REFERENCES

Belyashov V.A. (1993). 'Method for calculating ice loads encountered by propeller blades'. Proc. 12th Int. Conf. on Port and Ocean Eng., POAC-93, Hamburg, Vol. **2**, pp.359-368.

Hirt, C.W.; Nichols, B.D. (1981). 'Volume of fluid (VOF) method for the dynamics of free boundaries'. Journal of Computational Physics. **39** (1): pp. 201–225.

Menter F.R. (1994). 'Two equation eddy-viscosity turbulence models for engineering applications' AIAA Journal **32**: pp. 1598-1605.

Menter F.R., Langtry R.B., Likki S.R., Suzen Y.B., Huang P.G., Völker S. A. (2006). 'Correlation-based Transition Model using Local Variables. Part 1: Model Formulation', ASME J. Turbomachinery **128**, No. 3: pp. 413-422.

Rayleigh, Lord (1917). 'On the pressure developed in a liquid during the collapse of a spherical cavity'. Phil. Mag. **34**: pp. 94–98.

Sauer, J. (2000). 'Instationaer kavitierende Stroemungen - Ein neues Modell, basierend auf Front Capturing VOF und Blasendynamik', Dissertation, Universitaet Kalrsruhe.

Shur, M.L., Spalart, P.R., Strelets, M.Kh. and Travin, A.K. (2008). 'A hybrid RANS-LES approach with delayed-DES and wall-modelled LES capabilities'. International J. Heat and Fluid Flow **29**(6): pp. 1638-1649.

Taranov A. and Lobachev M. (2015). 'Influence of the Laminar-Turbulent Transition on the Accuracy of the Propeller Characteristics Prediction in the Model Scale', Proceedings of the 2015 International Conference on Mechanics - Seventh Polyakhov's Reading, ISBN 978-1-4799-6824-4/15, IEEE, pp. 1-4, http://ieeexplore.ieee.org/xpl/mostRecentIssue.jsp?punumber=7100634

Taranov A. (2015). 'Mesh convergence in calculations of flow around ice breaker propeller model', Proceedings of the Krylov State Research Centre **90**(374): pp. 55-62 (in russian).

DISCUSSION

Question from John Carlton

Have you developed any limits for chamfering on the blade section?

Author's closure

Yes, there some limits for this procedure developed in our research centre, which depends on propeller geometry and its ice class. But in present study the chamfering does not varied.